A Novel and Compact Optical Polarizer Incorporating a Layered Waveguide Core Structure

M. Rajarajan, *Member, IEEE*, B. M. A. Rahman, *Senior Member, IEEE*, and K. T. V. Grattan

***Abstract*—A compact optical polarizer based on a directional coupler incorporating layered waveguide core structures is studied in detail in this paper. Important waveguide design parameters such as the guide width, guide separation, guide height, refractive index contrast, and wavelength dependence have been analyzed by using the vectorial H-field finite-element method. The optical power transfer characteristics have been calculated by using the least squares boundary residual methods.**

***Index Terms*—Birefringence, finite-element method (FEM), integrated optics, optical polarizers.**

I. Introduction

SPATIAL TE/TM polarization splitters are important integrated components for polarization diversity optical systems, such as polarization diversity receivers for coherent detection. Polarization splitters have been studied by various researchers using a range of operating techniques. Asymmetric Y-branches on $LiNbO_3$ have been reported in which the effective indexes were electrooptically controlled [1]. Those based on metal-clad directional couplers in InGaAsP/InP have been demonstrated [2], [3], as have multimode interference (MMI) Mach–Zehnder interferometer (MZI)-based polarization splitters [4] where one arm of the Mach–Zehnder branch was covered with a metal layer to obtain different relative phase differences between the two arms for the two polarizations. The other techniques include a short section of proton exchanged waveguide [5] and an anisotropic overlay [6].

The analysis methods used to study the characteristics of these optical polarization splitters can be classified as either analytical or numerical methods, where analytical methods used may be accurate only for one-dimensional structures. However, most practical guided-wave devices must be considered as two-dimensional, and thus for the accurate design and characterization of these devices, a rigorous numerical tool is often the most viable solution. In this paper, the powerful and versatile finite-element method (FEM) and the least squares boundary residual (LSBR) methods have been used to calculate the modal properties and the excited modal coefficients at the junction, respectively, in such systems.

In this paper, we present a novel and compact directional coupler based optical polarizer incorporating thin layered regions and study their optimum fabrication parameters and the propagation characteristics of such structures.

Manuscript received October 29, 2002; revised July 22, 2003.

The authors are with the Photonics Research Group, School of Engineering and Mathematical Sciences, City University, Northampton Square, EC1V 0HB London, U.K. (e-mail: R.Muttukrishnan@city.ac.uk).

Digital Object Identifier 10.1109/JLT.2003.821750

II. Finite-Element and Least Squares Boundary Residual Methods

In the design and optimization of photonic devices, numerical methods are required to determine accurately the propagation characteristics of the allowed waveguide modes, including the extraction of complex propagation constants for waveguides with loss or/ and gain. The finite-element method has emerged as one of the most successful numerical methods for the analysis of high-frequency practical optical waveguide problems, because of its accuracy, flexibility, and versatility. The FEM is capable of analyzing structures with arbitrary shapes, index profiles, nonlinearities, and anisotropies. The vector $\mathbf{H}$-field variational formulation has been widely used to analyze practical optical waveguides in GaAs and InP material based systems [7]. In this paper, the above-mentioned attractive features of this method are utilized to optimize the polarizer design especially in the TE/TM ratio and device length calculations.

Although the FEM can be used to calculate the propagation constants and the modal field profiles, alone it cannot be used to analyze discontinuity along a guided-wave device or optoelectronic subsystem. Hence the LSBR method may be used to calculate the transmitted and the reflected coefficients at a discontinuity junction. Most research workers in this field use the simple overlap integral (OI) method to calculate the excited modal coefficients. However, this method can only consider one mode in each side of the discontinuity plane and also cannot consider the reflection. The fundamental boundary condition at the discontinuity plane is the continuity of the transverse components of both the electric ($\mathbf{E}$) and magnetic ($\mathbf{H}$) fields. This LSBR method is rigorously convergent [8], satisfying the boundary conditions in the usual least squares sense over the interface, and the error minimization is global rather than sampled. For directional coupler-based devices, at the discontinuity interface the even and the odd supermodes are generated to satisfy the necessary boundary conditions.

III. Directional Coupler Based Optical Polarizer

It is known that the propagation constants (β) for TE and TM are similar but not exactly the same. Similarly, the coupling lengths for the TE and TM polarizations are also similar but not exactly same. Although a simple directional coupler shows a polarization-dependent performance, however, the use of its TE/TM extinction is not sufficient in the design of an effective optical polarizer. It is known that layered structure regions show a different equivalent index for two polarizations; however, this difference of equivalent indexes is also not sufficient to enable the design of an optical polarizer incorporating two identical

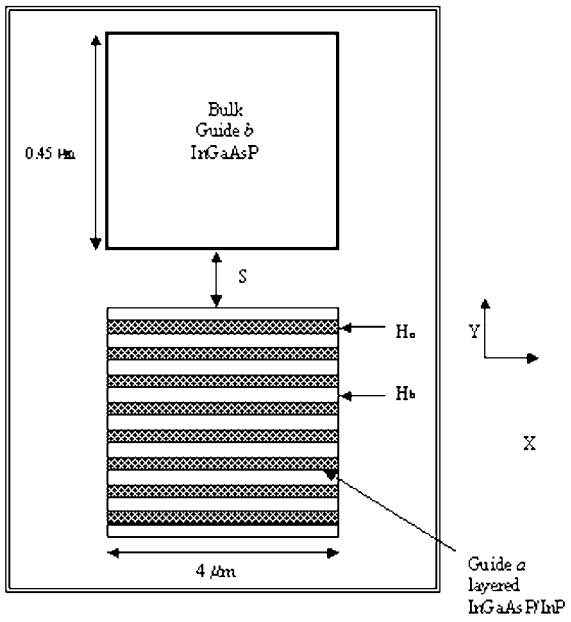

Fig. 1. The cross-section of the layered structure with nonidentical guides.

layered waveguide cores. In this paper, two nonidentical waveguides with one incorporating the layered region are used for the design of the polarizer. Although the finite-element method can be used to represent the layered core exactly, however, it has been shown by Rahman *et al.* [9] that the equivalent index approach might be acceptable to represent the layered region to reduce computational costs.

The cross-section of the directional coupler structure considered in this paper is shown in Fig. 1. The two guides a and b are separated by a distance S between the guides. The guides could be placed laterally; however, the structure considered here may be more suitable for fabrication if they are placed vertically. A single mask of width W can be used to fabricate both the waveguides. The lower guide a is a layered structure compressing nine periods of layer thickness of 25 nm. Initially a single waveguide incorporating sandwiched InGaAsP and InP layers completely burried in an InP substrate is considered for the simulation. The thickness of the InGaAsP (H_1) and InP (H_2) layers is 25 nm and the corresponding refractive indexes were taken as 3.4636 and 3.1717, respectively, at a bandgap wavelength of 1.48 μm. The operating wavelength was taken as 1.52 μm. It can be shown that the modal birefringence is highest when alternating layers have equal thickness. The width of the waveguide was fixed at 4 μm for this simulation work unless otherwise stated. For computational efficiency, a two-fold symmetry (thus considering only one-quarter) is exploited. A total of 16 000 elements were used to represent this structure. By representing each layered region exactly in the FEM, the effective index values ($\beta/\mathrm{k_o}$) for the quasi-TE and quasi-TM modes were calculated as 3.229 25 and 3.218 40, respectively. This illustrates a very high level of modal birefringence in such layered structures. To proceed, the entire layered core region has been replaced by a single homogeneous region with its equivalent index, calculated by using the equations in [9] and [10]. By substituting the values in the above equations, the equivalent index for the TE and TM polarizations was calculated as 3.3201 and 3.3080, respectively. When these equivalent indexes were used to replace the layered core region, the modal solutions obtained by the FEM yielded effective index values (n_e) of 3.224 84 and 3.214 62, respectively, for the TE and the TM polarizations. This small difference is due to the small number of layers used, which gives slight extra weight to high index region (as the ratio being 5:4). This clearly shows an underestimate of the propagation constants for both the polarizations when the equivalent index is used, particularly when a small number of layers are used. Next, the equivalent indexes for both the polarizations were adjusted to obtain the same effective indexes as were obtained for the exact representation of the layered core region. The corrected indexes were calculated to be 3.3274 and 3.3151 for the TE and the TM polarizations, respectively. The improved equivalent index is used rather than their exact representation, as for the coupled structure, not only the structure is more complex but also only one fold of symmetry can be used to enhance numerical efficiency. The upper guide b could be fabricated from bulk $\mathrm{In_{1-x}Ga_xAs_yP_{1-y}}$ material and by adjusting the molar fractions, the refractive index of the top guide can be made equal to 3.3274 (same as the equivalent index for TE mode in guide a) as guide b being homogeneous for both the TE and TM polarizations will see the same index.

IV. Analysis of the Results

The vector finite-element method is initially used to find the modal properties of the directional coupler structure. For the TM polarization, the two guides are nonidentical, and hence they are not phase matched. The height (H) and width (W) of the waveguides were taken as 0.45 and 4 μm, respectively.

Fig. 2(a) and (b) shows the dominant H_y field profiles of the TE supermodes. Since the two guides are identical for the TE case, the supermodes are either completely symmetrical or antisymmetrical. However, for the TM case, the two guides are nonidentical. The supermode field profiles (H_x) for the TM polarization are shown in Fig. 2(c) and (d). It can be noticed that for the even-like TM supermode, most of the power is in guide b and there is very little power in guide a, since TE wave sees a higher index in the upper guide.

From the modal solutions, the coupling lengths for the TE and the TM polarizations can be calculated. Fig. 3 shows the coupling lengths as a function of the guide separation for the TE and the TM polarizations. The solid and the dashed lines in Fig. 3 represent the TE and TM polarizations, respectively. The TE and the TM coupling lengths are defined as L_{cTE} and L_{cTM}, respectively, in Fig. 3. The coupling length axis is plotted in semilog scale to reveal the exponential variation of the coupling length for the TE polarization. As can be seen from Fig. 3, as the separation between the guides is increased from 0.5 to 1.5 μm, initially the TM curve (dashed) increases exponentially (linearly in a semilog scale). However, with further increase of separation, the TM curve reaches the maximum value asymptotically. At higher separations, the guides are nearly isolated, and with the waveguides being nonidentical, the propagation difference does not change considerably (maximum difference $\beta_{\mathrm{a}} - \beta_{\mathrm{b}}$, where β_{a} and β_{b} are the propagation constants of the

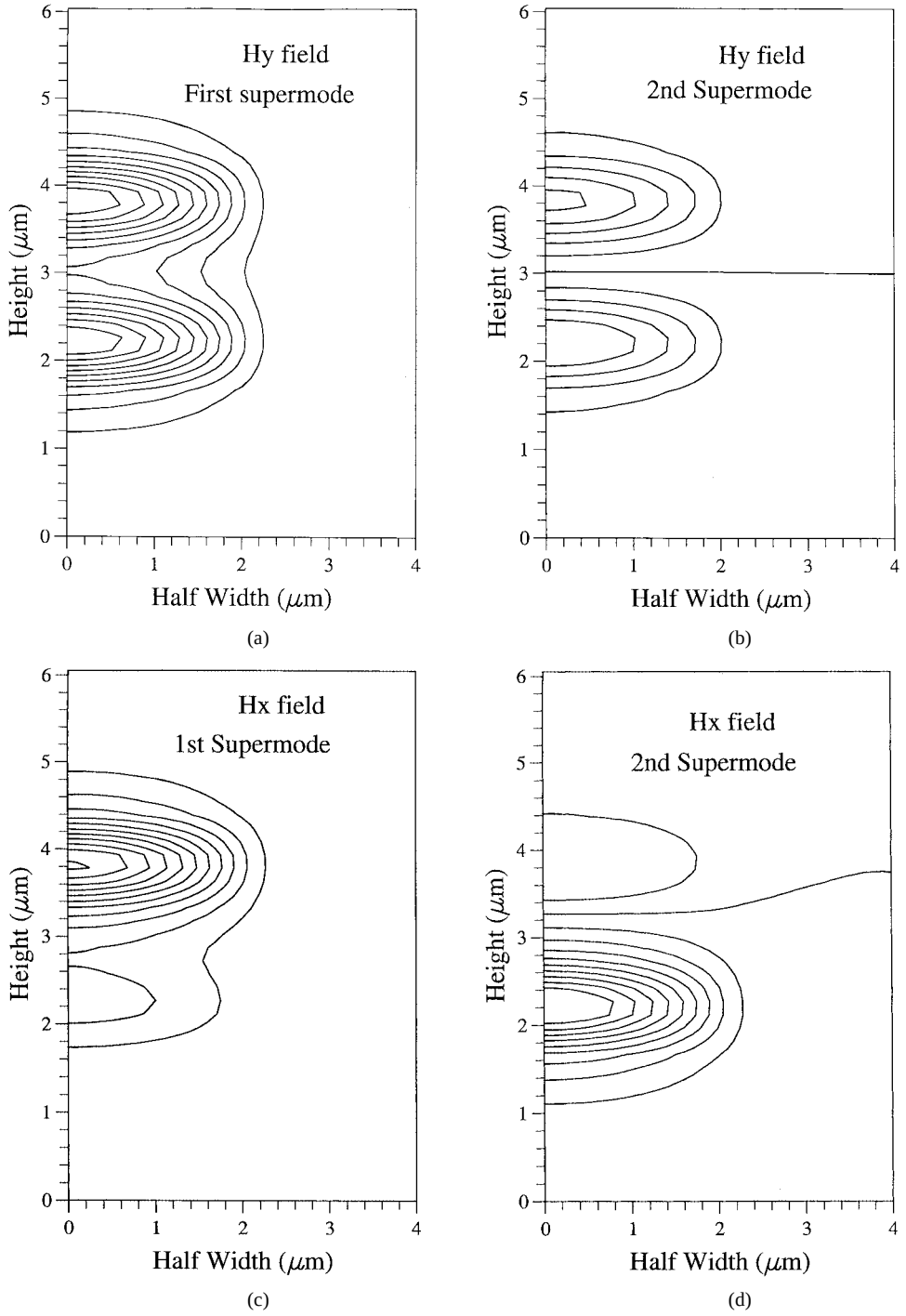

Fig. 2. H_y field profile of (a) the first TE supermode and (b) the second TE supermode. The H_x field profile of (c) the first TM supermode and (d) the second TM supermode.

isolated waveguides) with increasing separation and the coupling length remains constant. From Fig. 3, a design relationship can be achieved such that the coupling length of TE polarization is twice that of the TM polarization. In Fig. 3, the right-hand Y-axis shows the TE/TM coupling length ratios. It can be noticed from this figure that when the separation between the guides is 1.16 μm, the coupling length of the TE polarization is twice that of the TM polarization. The coupling lengths of the TE and the TM polarizations were calculated as 172.2 and 86.1 μm, respectively. Therefore, by fabricating a directional coupler section of 172.2 μm length, an effective compact TE/TM polarization splitter can be realized. In this design, the directional coupler parameters are selected in such a way that for TE polarization, the two guides are identical and hence they are phase matched.

Next, using the propagation constants and field profiles generated using the finite-element method, the LSBR method can be used to calculate the excited modal coefficients and from which the composite field profiles along the propagating z-direction can be obtained. Fig. 4(a) and (b) shows the composite

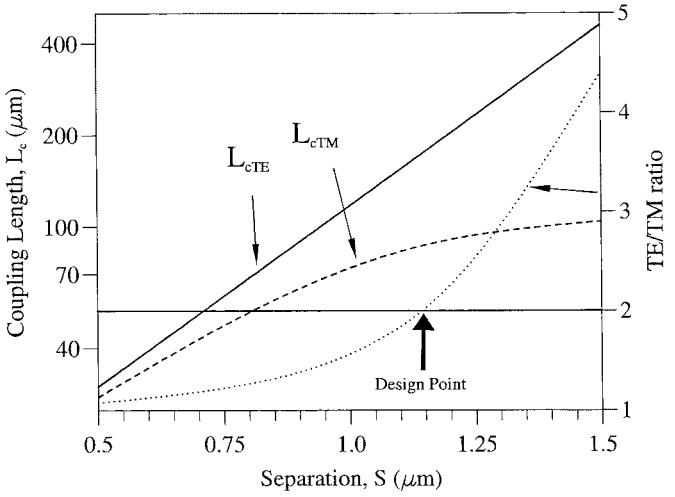

Fig. 3. Variation of the coupling length with the guide separation S.

field profiles at $z = 0_+$ μm and at $z = 172.2$ μm for the TE polarization. It can be noticed from Fig. 4(a) and (b) that initially most of the butt-coupled power is in the top guide b and evanescently coupled to the lower guide a at a coupling length of 172.2 μm. Fig. 4(c) shows the field profile at twice the coupling length, where it can be noticed that the power couples back to the top guide b. Fig. 4(d)–(f) shows the composite field profiles at $z = 0_+$ μm, $z = 85.1$ μm, and 172.2 μm for the TM polarization. It can be noticed from Fig. 4(d) initially that most of the optical power is butt-coupled in the top guide b. However, it can be noticed from Fig. 4(e) that only a fraction of the input power launched has transferred to the adjacent lower guide at one coupling length. As the power in the supermodes is not equally distributed for both the even and the odd supermodes, there is an incomplete power transfer at one coupling length for the TM case. It also verifies that when the guides are not phase matched, power cannot be coupled completely from one guide to the other. Fig. 4(f) shows the power transfer at twice the coupling length for the TM polarization. It can be noticed that the small fraction of the power, which was transferred at one coupling length, is now transferred back to guide b at twice the coupling length. Therefore, by designing a directional coupler of 172.2 μm length, both the TE and the TM polarizations can be split into the *cross* and *bar* ports, respectively.

Fig. 5 shows the variation of the power coupling as a function of the propagating distance Z. The transmitted coefficients are 0.708 71 and 0.705 39 for the TE even and the odd modes, respectively. The reflected coefficients are 0.550 156E-4 and 0.137 61E-4 for the TE even and odd modes. For the TM polarization, the transmitted and reflected coefficients for the even and odd modes are 0.993 46 (even), 0.114 02 (odd) and 0.187 18E-4 (even), 0.791 87E-5 (odd), respectively.

Although this device length can give a very attractive polarizer, it is always necessary to study their fabrication tolerances in order to understand their suitability for practical applications. Initially, the separation between the guides is varied from the design value of 1.16 to 1.2 μm, and its effects on the power transfer characteristics are studied in detail. The solid and the dashed lines show the TE and TM power transfer characteristics, respectively. The solid line shows the TE power transfer characteristic for guide a and the solid line with markers shows the TE power transfer characteristics for guide b. The dashed line shows the TM power transfer characteristics of guide a and the dashed line with markers shows the TM power transfer characteristics of guide b. As can be seen from this figure, at $z = 0_+$ μm for both the TE and TM polarizations, most of the power is in guide a, and there is almost zero power in guide b. However, at $z = 172.2$ μm, most of the TE and TM polarized power is in guides b and a, respectively. Therefore, by carefully selecting the device parameters, a passive TE/TM polarizer can be designed by incorporating a layered region without introducing surface plasmon modes, which are inherently lossy [3].

The dashed-dotted and the dotted curves show the power transfer characteristics for the nonideal case when the separation is slightly increased to 1.2 μm. The dashed lines (with and without markers) show the power in guides a and b, respectively, for the TE case. The dotted lines (with and without markers) show the power in guide a and b, respectively, for the TM case.

It can be noticed from these curves that even a small change in separation can deteriorate the power transfer characteristics. This phenomenon can be explained with the help of Fig. 3. It can be noticed from Fig. 3 that as the separation is increased above the design value of 1.16 μm, the coupling length will increase for both the TE and TM polarizations. This will destroy the "$2^* L_{\mathrm{cTM}} = L_{\mathrm{cTE}}$" relationship and hence will contribute to the deterioration of the power transfer characteristics. It can also be noticed that as the coupling lengths are increased slightly, the maximum power transfer point has slightly moved away from the design value of 172.2 μm. However, due to the phase mismatch, only 14% of power initially transferred to guide a and there is around 86% remaining power in the guide at the coupling for the TM case, although there is around 99% power transfer for the TE case at the coupling length. This is due to the fact that for the TE case, the guides are phase matched (but length is not matched to L_c) and for the TM case, they are not phased matched. Hence increasing the separation increases the TM mismatch further and hence deteriorates the performance of the TM polarization.

Next, the fabrication tolerance on the guide width of the directional coupler section is studied. Fig. 6 shows the variation of the power coupling as a function of the distance Z. The solid and the dashed lines show the TM and TE polarization powers in guide a for a guide width of 4 μm. The solid and the dashed lines with markers show the TM and TE polarization powers in guide b for a guide width of 4 μm. The dashed-dotted line and the dotted line show the TE and TM polarization powers in guide a, respectively, for a guide width of 3.6 μm. The dashed-dotted and the dotted lines with markers show the TE and TM polarization powers in guide b, respectively, for a guide width of 3.6 μm. Finally, the dashed-dotted line with and without markers shows the TE power transfer characteristics for a guide width of 3 μm.

It can be noticed from Fig. 6 that there is hardly any noticeable difference in the power transfer characteristics when the width is reduced from 4.0 to 3.6 μm. However, as the width is reduced further to 3 μm, only then there is some noticeable difference,

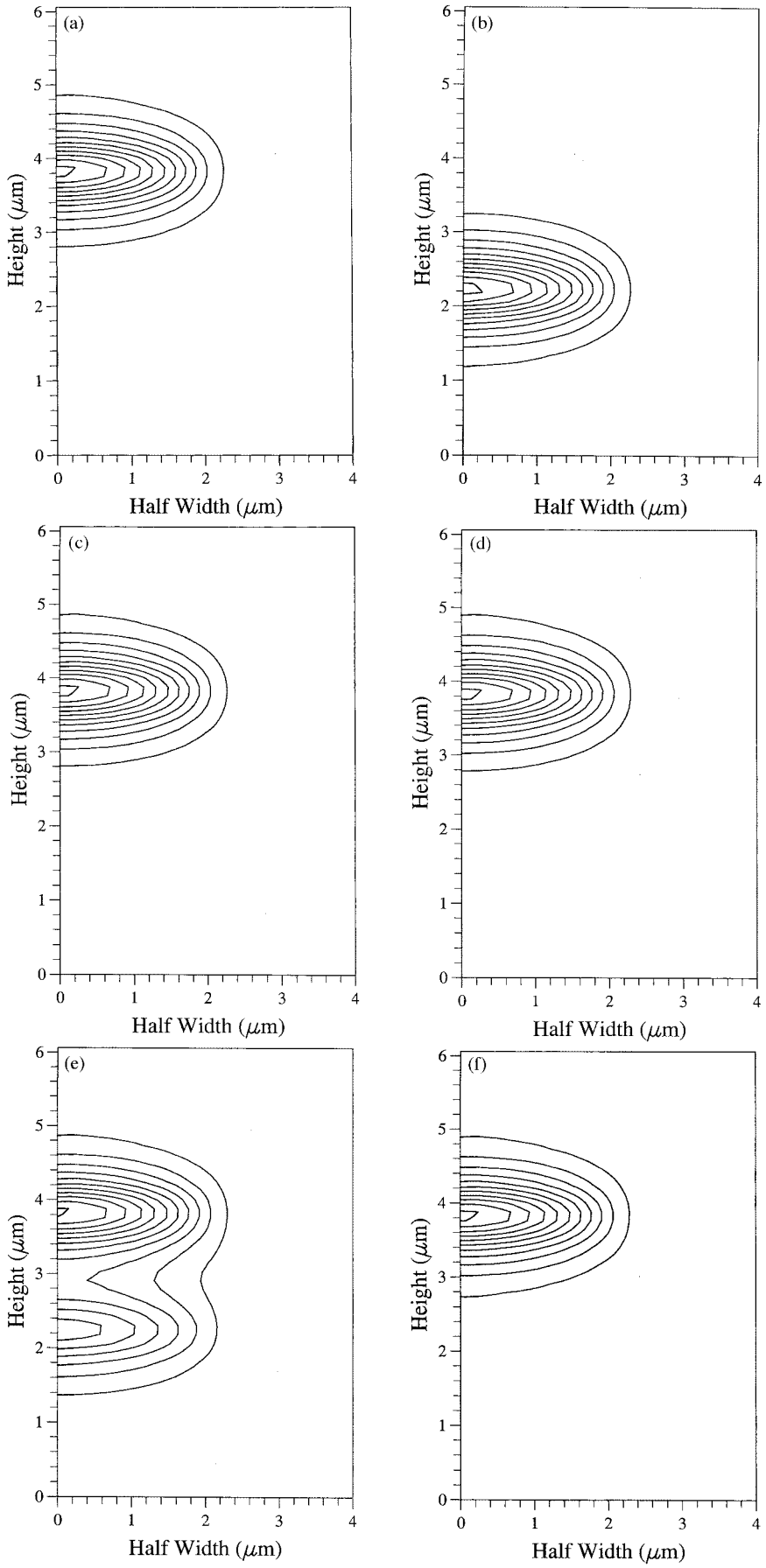

Fig. 4. Composite field profile of the TE modes at (a) $z = 0_+$, (b) modes at $z = 172.2$ μm, and (c) $z = 344.4$ μm Composite field profile of the TM modes at (d) $z = 0_+$, (e) $z = 85.1$ μm, and (f) $z = 172.2$ μm.

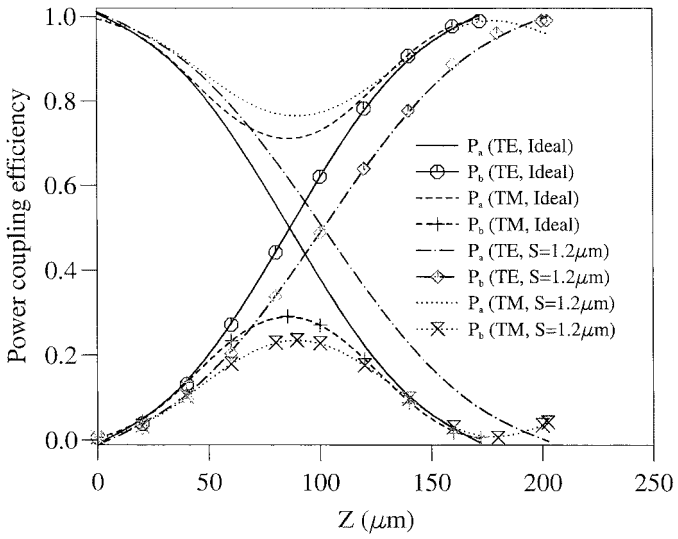

Fig. 5. Variation of the power coupling as a function of the propagation distance for a guide separation of 1.2 μm.

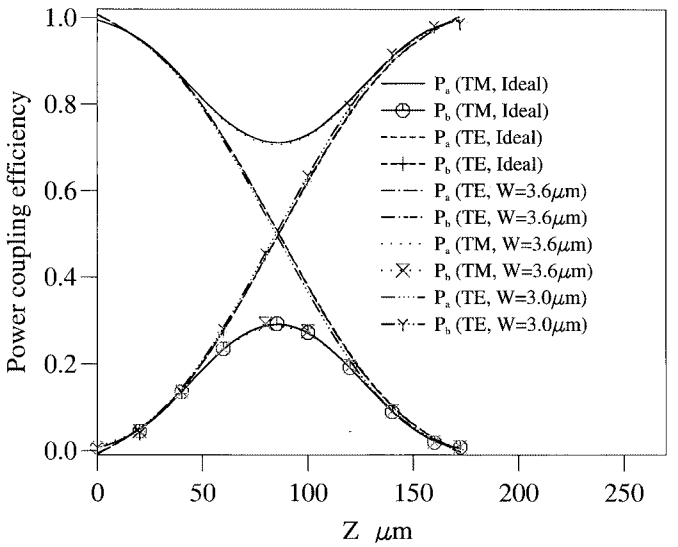

Fig. 6. Variation of the power coupling along the axial direction for different waveguide widths.

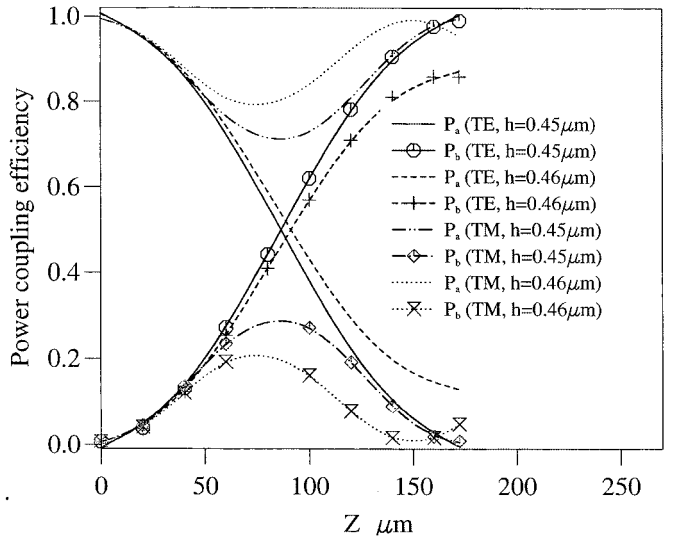

Fig. 7. Variation of the power transfer characteristics as a function of the propagation distance for a top guide height of 0.46 μm.

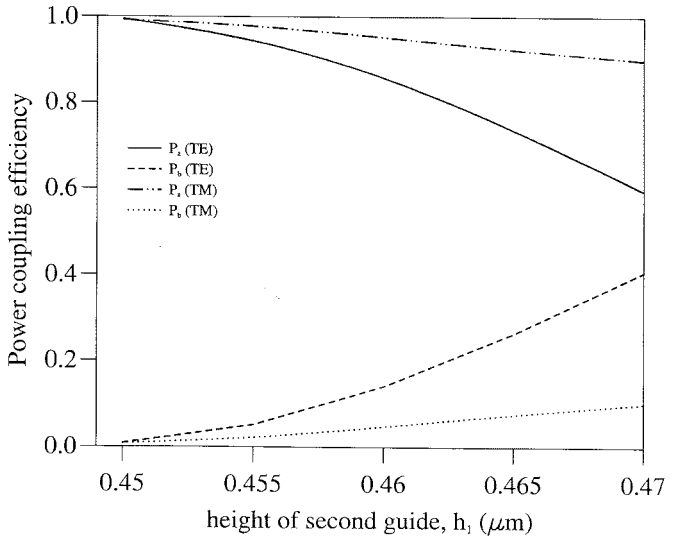

Fig. 8. Variation of the power coupling efficiency as a function of the second guide height.

although still very negligible and within the desired fabrication tolerances.

It is important to control the height of these waveguides within a few nanometers, and the sensitivity of this parameter is studied next. The height of the top guide b is increased from 0.45 to 0.46 μm. The power transfer characteristics are shown in Fig. 7 as a function of the propagation distance Z. The solid lines (without and with markers) show the power transfer characteristics for guides a and b, respectively, for the TE polarizations for the ideal case. The dashed lines (without and with markers) show the power transfer characteristics for the TE polarization for the nonideal case when the height of the top guide b is increased from 0.45 to 0.46 μm. The dashed-dotted lines (without and with markers) show the TM power transfer curve for guides a and b, respectively, for the ideal case. The dotted curves (without and with markers) show the power transfer characteristics for guides a and b, respectively, for the nonideal case. It can be noticed from these curves that the deterioration of the TM power transfer characteristics is more severe than the TE case. This can be explained by using the same argument as discussed before. As the height of one waveguide is increased, the guides are no longer identical and this will make the TM case worse. However, if the heights of both the waveguides are modified by similar values, the performance of the polarizer is expected to be satisfactory.

It is important to understand the crosstalk of these structures, and this is shown in Fig. 8. Fig. 8 shows the power coupling efficiency as a function of the second guide height. The solid and the dashed lines show the power in the bar (P_{a}) and cross (P_{b}) ports, respectively, for the TE case for different guide heights. The dashed-dotted and dotted lines show the power in the bar and the cross states, respectively, for the TM polarization for different guide heights. It can be noticed that as the second guide height is increased from the design value of 0.45 μm, the crosstalk increases. From Fig. 8, it can also be noticed that increasing the

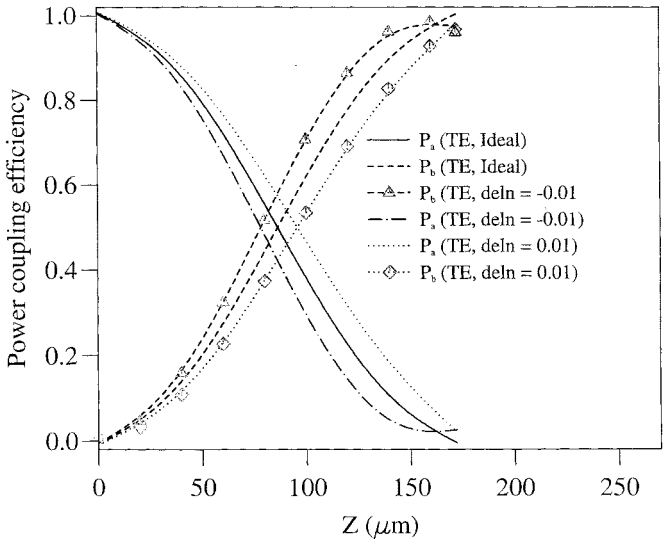

Fig. 9. Power coupling efficiency as a function of the propagation distance for different index contrasts (deln) for the TE polarization.

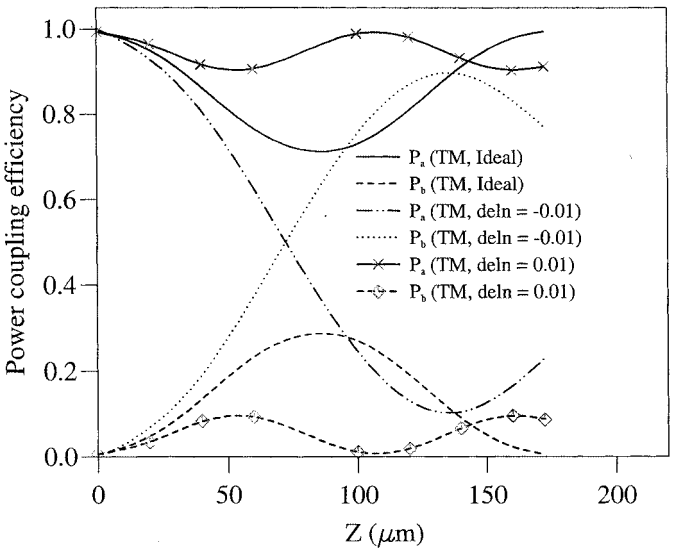

Fig. 10. Variation of the power transfer characteristics as a function of the propagation distance for different index contrasts for the TM polarization.

height by as little as 10 nm can deteriorate the power transfer characteristics by 20%. However, increasing the height by 20 nm to 0.47 μm has considerable effect, and the resulting power coupling efficiency can be as low as 60% compared to 99.9% for the ideal design. This shows that the fabrication tolerance has to be within 10-nm range to avoid performance degradation. Although this value sounds a bit tight on the fabrication tolerances, it has been indicated by previous research workers that the fabrication control on the waveguide height is less of an issue than the other parameters, such as the width.

Next the effect of index contrast on the power transfer characteristics is illustrated. Fig. 9 shows the effect of refractive index contrast (deln) on the power coupling efficiency for the TE and the TM polarizations. The refractive index contrast (deln) is defined as the difference between the core and the substrate refractive index values. The solid and the dashed lines show the TE and TM power transfer characteristics. It can be noticed

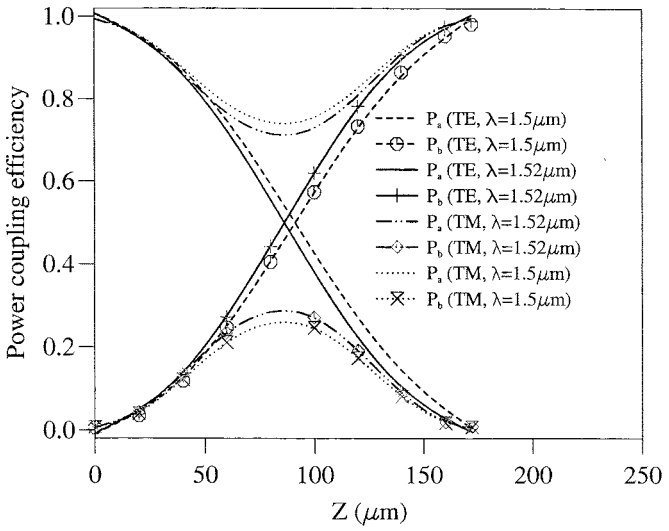

Fig. 11. Power coupling efficiency as a function of the propagation distance for three wavelengths.

for the TE polarization that when the index contrast is reduced from the ideal case by 0.01 for both the guides, then the power transfer curve (dashed line with markers) is slightly above the ideal curve (dashed). However, if the refractive index contrast is increased by 0.01 for both the guides, then the power transfer characteristic is slightly below the ideal case (dotted curve with markers). However, the effect is more critical for the TM case, and Fig. 10 shows the power transfer characteristics as a function of the propagation distance. It can be noticed that when the refractive index contrast is increased by 0.01, then the power transfer characteristics (dashed line with markers) deteriorates considerably from the ideal case (solid) as the phase mismatch is increasing further. However, if the refractive index contrast is reduced by 0.01, then the power transfer characteristic (dotted line) deviates from the ideal case has better characteristics than the previous case. This is due to the fact that as the refractive index contrast is reduced, the guides are moving closer to the phase matching condition and hence is following almost a similar pattern.

Next the wavelength sensitivity of these devices is studied. Fig. 11 shows the power coupling efficiency as a function of the propagation distance Z for two wavelengths. The solid lines (without and with markers) show the TE power transfer characteristics for guides a and b, respectively, for a wavelength of 1.52 μm. The dashed lines (without and with markers) show the TE power transfer characteristics for guides a and b at a wavelength of 1.5 μm. The dashed-dotted lines (without and with markers) show the TM power transfer characteristics for guides a and b, respectively, at a wavelength of 1.52 μm. The dotted lines (without and with markers) show the TM power transfer characteristics for guides a and b at a wavelength of 1.5 μm.

It can be seen from Fig. 11 that a slight change in the wavelength can deteriorate the power transfer characteristics slightly. At the design wavelength of 1.52 μm, the crosstalk is 20 dB, which could be taken as a satisfactory design. However a wavelength tolerance of $\pm$20 nm can be achieved at an additional crosstalk penalty of 3 dB. A wider window of tolerance of $\pm$40 nm can be achieved at an additional crosstalk penalty of 6 dB.

This bandwidth is reasonably large enough for many practical applications, including that for dense WDM systems.

V. Summary

In this paper, the authors have shown a novel design of polarization splitter without using the metal clad or anisotropic material. The modal birefringence of a layered structure is exploited to design a compact directional coupler-based polarization splitter. Nonidentical guides are designed in such a way that they are phase matched for TE but not for the TM polarizations. Device parameters are designed in such a way that the device length is equal to odd or even multiple of the coupling length for different polarizations. Important fabrication parameters such as the width, height, separation, refractive index contrast, and wavelength sensitivity have been rigorously verified, and their operating characteristics shown. It can be summarized from these fabrication results that this compact polarizer is more sensitive to height, index contrast, and guide separation but reasonably robust with the waveguide width and the operating wavelength variations.

References

[1] Y. P. Liao, R. C. Lu, C. H. Yang, and W. S. Wang, "Passive Ni:$LiNbO_3$ polarization splitter at 1.3 μm wavelegth," *Electron. Lett.*, vol. 32, pp. 1003–1005, 1996.

[2] P. Albrecht, M. Hamacher, H. Heidrich, D. Hoffmann, H. P. Nolting, and C. M. Weinert, "TE/TM Mode Splitter on InGaAsP/InP," *IEEE Photon. Technol. Lett.*, vol. 2, pp. 114–115, 1990.

[3] M. Rajarajan, C. Themistos, B. M. A. Rahman, and K. T. V. Grattan, "Characterization of metal-clad TE/TM mode splitters using the finite element method," *J. Lightwave Technol.*, vol. 15, pp. 2264–2269, 1997.

[4] M. H. Hu, J. Z. Haung, R. Scarmozzino, M. Levy, and R. M. Osgood, "Tunable Mach-Zehnder polarization splitter using height tapered Y-branches," *IEEE Photon. Technol. Lett.*, vol. 9, pp. 773–775, 1997.

[5] S. Uehara, T. Izawa, and H. Nakagome, "Optical waveguide polarizer," *Appl. Opt.*, vol. 13, pp. 1753–1757, 1974.

[6] P. G. Suchoski, T. K. Findakly, and F. J. Leonberger, "Low-loss high-extinction polarizers fabricated in $LiNbO_3$ by proton exchange," *Opt. Lett.*, vol. 13, pp. 172–174, 1988.

[7] B. M. A. Rahman and J. B. Davies, "Finite-element analysis of optical and microwave waveguide problems," *IEEE Trans. Microwave Theory Tech.*, vol. MTT-32, pp. 922–928, 1984.

[8] ——, "Analysis of optical waveguide discontinuities," *J. Lightwave Technol.*, vol. 6, pp. 52–57, 1988.

[9] B. M. A. Rahman, Y. Liu, and K. T. V. Grattan, "Finite-element modeling of one- and two-dimensional MQW semiconductor optical waveguides," *IEEE Photon. Technol. Lett.*, vol. 5, pp. 928–931, 1993.

[10] G. M. Alman, L. A. Molter, H. Shen, and M. Dutta, "Refractive index approximations from linear perturbation theory for planar MQW waveguides," *J. Lightwave Technol.*, vol. 28, pp. 650–657, 1992.

M. Rajarajan (M'03), photograph and biography not available at the time of publication.

B. M. A. Rahman (S'80–M'82–SM'93) received the B.Sc.Eng. and M.Sc.Eng. degrees in electrical engineering with distinction from the Bangladesh University of Engineering and Technology (BUET), Dhaka, Bangladesh, in 1976 and 1979, respectively, receiving two gold medals for being the best undergraduate and graduate student of the university in these two years. In 1979, he was awarded with a Commonwealth Scholarship to study for the Ph.D. degree in the U.K. and, subsequently, in 1982, received the Ph.D. degree in electronics from University College London, London, U.K.

From 1976 to 1979, he was a Lecturer at the Electrical Engineering Department, BUET. In 1982, after receiving the Ph.D. degree, he joined University College London as a Postdoctoral Research Fellow and continued his research work on the development of the finite-element method for characterizing optical guided-wave devices. In 1988, he joined City University, London, U.K., as a Lecturer. Currently, he is Professor and Assistant Dean of Engineering. At City University, he leads the research group on photonics modeling, specializing in the use of rigorous and full-vectorial numerical approaches to design, analyze, and optimize a wide range of photonic devices. He has published more than 250 journal and conference papers, and his journal papers have been cited nearly 800 times.

Prof. Rahman is a Member of the Institution of Electrical Engineers (IEE), London, U.K., and the European Optical Society and is a Chartered Engineer.

K. T. V. Grattan, photograph and biography not available at the time of publication.